FUDMA Journal of Sciences (FJS)
ISSN online: 2616-1370
ISSN print: 2645 - 2944
Vol. 10 No. 23, December (Special Issue), 2026, pp 55 – 60
DOI: https://doi.org/10.33003/fjs-2026-1023-6627

Design and Experimental Characterization of a Circularly Slotted Hexagonal Ultra-Wideband Antenna for Microwave Breast Imaging

[*1]Isah Musa Danjuma, [2]Salamatu Abubakar Ibrahim and [2]Raed Abd Alhameed

[1]Department of Electrical Engineering, Nigerian Defence Academy, Kaduna, Nigeria
[2]Department of Engineering and Digital Technologies, University of Bradford, United Kingdom

*Corresponding authors' email: imdanjuma@nda.edu.ng

Received: 05 Nov. 2026
Accepted: 24 Nov. 2026
Published: 28 Nov. 2026

ABSTRACT
This study presents the design, fabrication and characterisation of a compact circularly slotted hexagonal ultra-wideband (UWB) antenna intended for microwave breast-imaging applications. The proposed antenna incorporates a circular slot within a hexagonal radiating patch to improve its impedance characteristics while maintaining a compact structure. The antenna is implemented on an FR-4 substrate with overall dimensions of 30 × 30 × 1.6 mm³ and is modelled using Computer Simulation Technology (CST). The simulated results indicate an impedance bandwidth of approximately 4–8 GHz, corresponding to an absolute bandwidth of 4 GHz and a fractional bandwidth of 66.7%. A minimum reflection coefficient of approximately −27 dB is obtained near 5.5 GHz. The measured and simulated reflection-coefficient responses show good agreement across the investigated operating band, supporting the antenna-level characterisation of the fabricated prototype. Although the achieved bandwidth provides wideband operation within a portion of the conventional UWB spectrum (3.1–10.6 GHz), it does not cover the entire UWB range. Furthermore, the present results establish antenna impedance performance but do not demonstrate tumour detection or diagnostic accuracy. Further investigation involving fully characterised tissue phantoms, quantitative radiation measurements and experimental image reconstruction is required to establish its performance in a complete microwave breast-imaging system.

Keywords: Circularly Slotted Antenna, UWB Antenna, Breast Cancer Imaging, Microwave Imaging

INTRODUCTION

Ultra-wideband (UWB) antennas have attracted considerable research interest because of their wide impedance bandwidth, compact structure, and potential for use in body-centric and biomedical microwave imaging systems. In these applications, antenna performance is particularly important because the antenna must transmit and receive electromagnetic signals in the presence of biological tissues. Previous studies have investigated UWB antenna configurations for body-centric imaging and related biomedical applications, demonstrating the importance of antenna geometry and impedance characteristics in the development of suitable imaging-system components (Danjuma et al., 2020; Rafique et al., 2022).

Conventional breast-imaging modalities, including mammography, ultrasound and magnetic resonance imaging (MRI), remain important tools for clinical assessment and diagnosis. Each modality has established applications, as well as practical limitations associated with factors such as radiation exposure, cost, accessibility and imaging performance in different breast-tissue conditions. Microwave breast imaging has therefore attracted attention as a potential complementary approach. It uses electromagnetic interactions with biological tissues and differences in their dielectric properties to obtain information that may contribute to breast assessment (Martellosio et al., 2016; Rafique et al., 2022). However, microwave imaging is still subject to technical and clinical validation challenges. It should consequently be considered a developing complementary technology rather than a proven replacement for conventional clinical imaging methods.

The antenna is an important component of a microwave imaging system because its impedance characteristics and electromagnetic behaviour influence signal transmission and reception. Designing an antenna for operation near biological tissues presents additional challenges, since tissue loading and dielectric properties can affect its performance. Previous work has considered different antenna configurations for body-centric imaging and breast-imaging applications (Danjuma et al., 2020; Abdulla & Demirkol, 2024). These studies provide a basis for further investigation of compact antenna geometries that can provide suitable impedance bandwidth for microwave breast-imaging systems.

In this study, the proposed antenna combines a hexagonal radiating patch with a circular slot, a 50 Ω microstrip feed line and a partial ground-plane configuration on an FR-4 substrate. The design-specific contribution is the investigation of this circularly slotted hexagonal configuration as a compact antenna structure, with attention to its impedance response over the 4–8 GHz operating band. The circular slot is incorporated as a geometrical modification of the hexagonal radiating element, while the feed and partial ground-plane dimensions are considered in the antenna design and optimisation. The resulting antenna has overall dimensions of 30 × 30 × 1.6 mm³. Its reported operating band is 4–8 GHz, which represents wideband operation over a portion of the conventional UWB spectrum (3.1–10.6 GHz), rather than coverage of the entire range.

This study aims to design, fabricate and characterise a compact circularly slotted hexagonal ultra-wideband antenna for microwave breast imaging, with particular emphasis on

impedance bandwidth and electromagnetic performance under tissue-loading conditions.

MATERIALS AND METHODS

Antenna Design and Configuration

The proposed antenna was designed as a compact planar structure comprising a hexagonal radiating patch with a circular slot, a 50 Ω microstrip feed line and a partial ground-plane configuration. The antenna was implemented on an FR-4 dielectric substrate with a relative permittivity of 4.6 and a thickness of 1.6 mm. The overall antenna dimensions are 30 × 30 × 1.6 mm³. This dimension is used consistently throughout the revised manuscript.

The circular slot is incorporated at the centre of the hexagonal radiating patch as a geometrical modification intended to influence the antenna's impedance characteristics. The microstrip feed line is connected to the radiating element and is designed for a nominal characteristic impedance of 50 Ω. A partial ground-plane structure is provided on the opposite side of the substrate. The ground-plane configuration and the gap between the feed line and ground plane are considered in the antenna design to obtain the desired impedance response. The principal geometrical parameters of the proposed antenna are summarised in Table 1. These include the substrate dimensions, patch dimensions, circular-slot diameter, feed-line dimensions, feed-transition parameter and partial ground-plane dimensions.

Table 1: Optimised Geometrical Parameters of the Proposed Antenna

Parameter	Subscription	Value(mm)
SW	Substrate Width	30
SL	Substrate Length	30
ST	Substrate Thickness	1.6
ML	Microstrip Length	11.40
MW	Microstrip Length	2.5
MG	Microstrip Gap	0.45
LS	Slot Dimension	11.49
SS	Side Length	9.33
2R	Circular Slot Diameter	8.6
a	Feed Transition Angle	25^0
GL	Ground Plane Length	11.10
GW	Ground Plane Width	13.35

Substrate and Material Properties

The antenna was designed using an FR-4 substrate with a relative dielectric permittivity of 4.6 and a thickness of 1.6 mm. These properties were used in defining the dielectric substrate for the electromagnetic model. The conductor was implemented using pure copper with a thickness of 1.6 mm. The dielectric loss tangent used in the simulation was 0.75.

Parametric Study and Design Optimisation

A parametric study was undertaken to examine the influence of selected geometrical parameters on the antenna response. The parameters considered included the partial ground-plane dimensions, feed configuration, substrate characteristics and circular-slot geometry. Particular attention was given to the ground-plane length and width, the feed-transition angle and the dimensions of the radiating patch and circular slot.

The ground-plane configuration was investigated because changes in its dimensions can influence the impedance response and operating bandwidth. The feed configuration was also considered because the transition between the microstrip feed line and the radiating patch affects impedance matching. In addition, the substrate was considered in relation to its dielectric properties and thickness.

The final geometrical values selected for the antenna are presented in Table 1. The optimisation objective was to obtain a compact antenna with an appropriate impedance response over the intended operating band. The final design produced an operating bandwidth of approximately 4–8 GHz, as discussed in the Results and Discussion section.

Electromagnetic Simulation

The proposed antenna was modelled and analysed using Computer Simulation Technology (CST). The software was used to evaluate the antenna's electromagnetic response, including its reflection coefficient (S_{11}), and to investigate the influence of the selected geometrical parameters.

The simulation was conducted using the following settings: CST version suite 2025; Time-Domain (FIT**)** solver type ; boundary conditions on Xmin, Xmax, Ymin, Ymax, Zmin and Zmax; excitation or port configuration One 50 Ω waveguide port; Hexahedral FIT mesh type and resolution ; and 0.02 dB between successive refinement passes as convergence criterion.

The simulated reflection coefficient was used to determine the impedance bandwidth of the antenna. The operating bandwidth was identified over the frequency interval within which the reflection coefficient satisfied the −10 dB criterion. The simulated response was subsequently compared with the measured response of the fabricated antenna as contained in Figure 4.

Antenna Fabrication and Experimental Measurement

The proposed antenna was physically implemented on an FR-4 substrate with overall dimensions of 30 × 30 × 1.6 mm³. The fabricated prototype was characterised experimentally, and its reflection-coefficient response was compared with the corresponding simulated result.

The measurement was performed using Rohde & Schwarz ZNB8 vector network analyser over the frequency range of 8.5 GHZ. The measurement arrangement used 50 Ω coaxial RF cable with an SMA male connector. Calibration was carried out using Short-Open-Load-Thru, with the measurement reference plane established at the end of the coaxial cable connected to the antenna's SMA connector. The measurement environment was carried out in the laboratory free space.

Breast Phantom Configuration

A breast phantom arrangement was considered to investigate the proposed antenna in a microwave breast-imaging configuration. As illustrated in Figure 5, four antenna sensors were arranged around a breast-mimicking phantom. The manuscript describes the use of low-cost materials to replicate tissue properties and the inclusion of a tumour-mimicking target.

The phantom configuration was also represented in the antenna-array simulation shown in Figure 6.

The human arm phantom consists of three tissue layers representing wet skin, fat, and muscle. The overall phantom dimensions are 50 mm × 50 mm × 400 mm, following a configuration similar to that reported in Danjuma, I. M., et al. The dielectric properties of the constituent tissue layers are defined using the relative permittivity and electrical conductivity values reported at 3.1 GHz.

Antenna Layout

The geometry of the proposed antenna consists of a hexagonal radiating patch centrally positioned on a dielectric substrate with overall dimensions of 30 × 30 x 16 mm^3 as shown in Fig. 1 and 2 respectively. This compact configuration is suitable for integration into portable biomedical imaging systems. The radiating element is modified by incorporating a circular slot at its center, which enhances surface current distribution, thereby improving impedance bandwidth and overall radiation performance across the ultra-wideband (UWB) frequency range. The radiating patch is exciting, a microstrip feed line with width MW and length ML, designed to achieve a characteristic impedance of 50 Ω for efficient power transfer. The feed line extends from the lower edge of the substrate and is directly connected to the patch, ensuring effective excitation and minimal signal reflection.

On the opposite side of the substrate, a partial ground plane configuration is implemented to further enhance bandwidth performance. This ground structure consists of two symmetrical rectangular sections defined by GL (ground length) and GW (ground width). A carefully optimized gap (P) between the feed line and the ground plane is introduced to improve impedance matching and to extend the operational bandwidth.

Key geometrical parameters governing the antenna performance include the side length of the hexagonal patch (SS), slot dimensions (LS and WS), and the effective size of the inner Circular slot (R). Additionally, the overall patch length (PL) and substrate length (SL) define the physical profile of the antenna. A small angular parameter (a°) at the feed junction is incorporated to facilitate smooth current transition between the feed line and the radiating element, thereby reducing return loss and enhancing radiation efficiency.

Overall, the proposed antenna layout provides a compact and planar configuration while maintaining improved impedance bandwidth and stable radiation characteristics. The combination of the circular slot, optimized feed structure, and partial ground planes contributes to reliable antenna performance, particularly when the antenna operates in close proximity to biological tissues. These characteristics make the proposed design a practical and promising candidate for ultra-wideband breast cancer imaging applications.

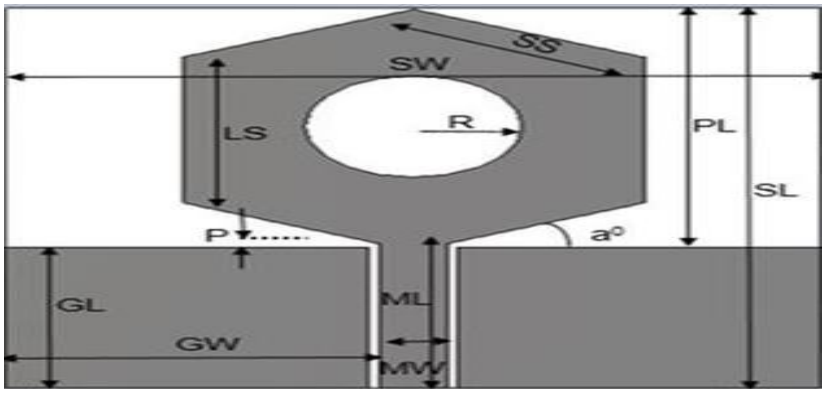


Figure 1: Geometric Configuration of the Antenna

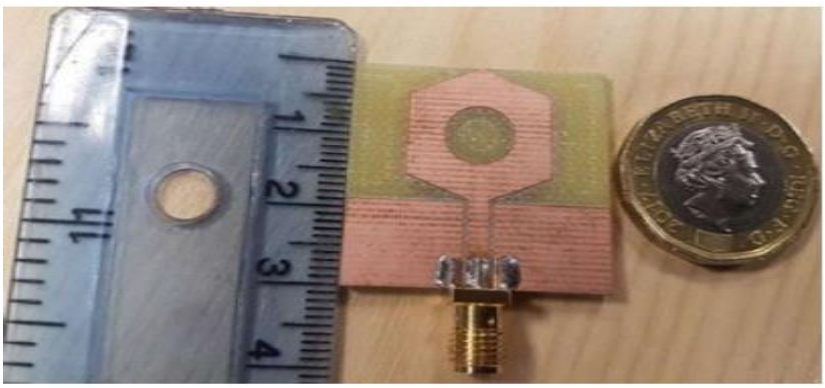


Figure 2: Physical Implementation of the Antenna

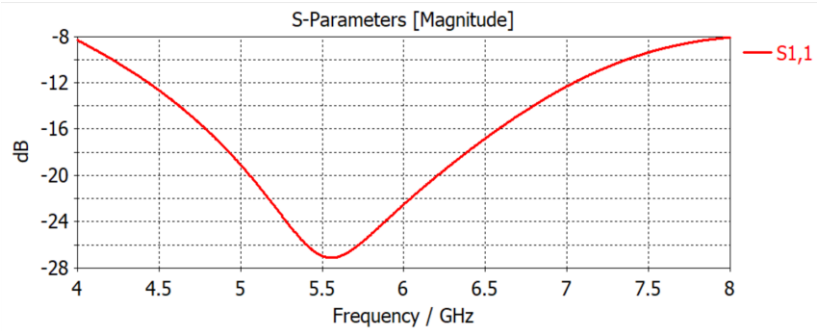


Figure 3: Simulation Results of the Proposed Sensor

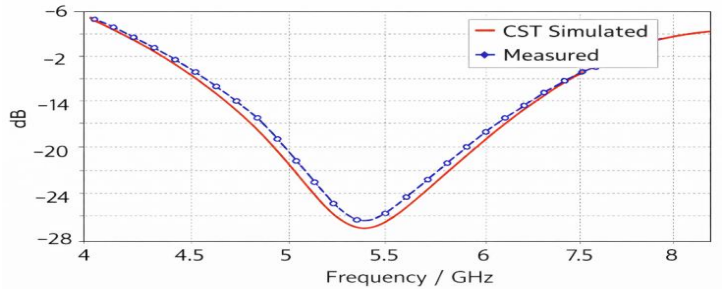


Figure 4: Simulation and Measured Results of the Proposed Sensor

Parametric Study

A parametric analysis was conducted to evaluate the influence of key design factors, including ground plane dimensions, feed point position, and substrate selection. This process was essential in optimizing the antenna performance for UWB biomedical imaging applications

Effect of Ground Plane Size

The antenna is fabricated on an FR-4 substrate (ε_r = 4.6, thickness = 1.6 mm) with overall dimensions of 30 × 30 mm². The study shows that the ground plane width has a greater impact on radiation efficiency, while its length primarily affects the lower cutoff frequency. Minor variations between simulated and measured results were observed, particularly at lower frequencies. Using consistent dimensions from the design ensured improved agreement between results, leading to enhanced gain and stable radiation performance suitable for biomedical applications.

Effect of Feed Point Position

The position and configuration of the feed line significantly influence impedance matching and overall antenna performance. A smooth transition between the microstrip feed and the radiating patch improves return loss and bandwidth. Results show that the reflection coefficient (S11) varies with feed position, making proper placement critical. Adjusting the feed angle also affects resonance: a 15° angle produces lower-frequency resonance, while increasing it to 25° shifts operation into the desired UWB range (around 3.1 GHz), although careful tuning is required to maintain good matching.

Effect of Substrate Choice

Substrate selection plays a key role in antenna performance near biological tissues. Lower permittivity materials reduce surface wave losses and improve radiation efficiency, while higher permittivity allows for more compact designs but may increase losses. Substrate thickness also affects performance: thicker substrates enhance bandwidth, whereas thinner ones improve impedance matching near the body. The chosen FR-4 substrate provides a practical balance between size, cost, and performance for biomedical use.

Simulation Environment and Validation

The antenna was modelled and optimized using CST software within a simplified human tissue phantom. Figure. 3 shows the simulated reflection coefficient (S_{11}) of the antenna. Key electromagnetic properties, such as permittivity and conductivity, were incorporated to simulate realistic conditions. Additional validation was performed using a breast phantom model with a tumour-mimicking inclusion with the 4 antenna sensors arranged around the breast mimicking phantom as shown in Figure. 5.

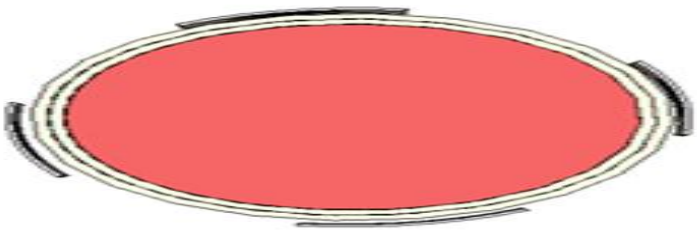


Figure 5: Proposed UWB Antenna Array Arranged Around the Breast Phantom

The experimental setup used common, low-cost materials to replicate tissue properties. Results show that the antenna maintains stable UWB performance across varying conditions and distances, demonstrating robustness for biomedical imaging applications as shown in Fig. 6.

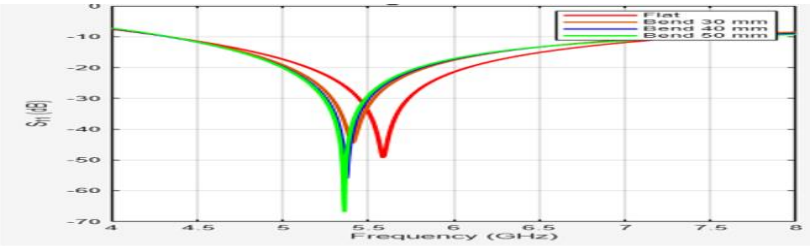


Figure 6: UWB Antenna Array Simulation Results Arranged Around the Breast Phantom

RESULTS AND DISCUSSION

The performance of the proposed Circularly slotted hexagonal antenna was evaluated using Computer Simulation Technology (CST). The key performance metrics, including reflection coefficient (S_{11}), impedance bandwidth, and radiation characteristics, were analysed to assess its suitability for breast cancer imaging applications. It is observed that the antenna achieves an impedance bandwidth ($|S_{11}| \leq -10$ dB) ranging from approximately 4 GHz to 8 GHz, corresponding to a bandwidth of about 4 GHz. A strong resonance is observed around 5.4–5.6 GHz, where the minimum S_{11} reaches approximately −27 dB, indicating excellent impedance matching at the resonant frequency.

A comparison between the simulated and measured results, as presented in Fig. 4, shows good agreement across the operating frequency range. Although some small differences can be observed, the overall trends are closely matched. This level of agreement indicates that the fabricated antenna performs largely as predicted during the simulation, thereby confirming the reliability of the proposed design and its suitability for the intended breast cancer imaging application. The achieved bandwidth, although not covering the full conventional UWB range (3.1–10.6 GHz), still falls within a wideband operational range suitable for microwave imaging applications.

The incorporation of the Circular slot plays a significant role in enhancing the impedance characteristics by improving surface current distribution and reducing reflection losses. The gradual slope of the S_{11} curve indicates stable impedance behaviour across the operating band. This stability is essential for consistent signal transmission and reliable imaging performance. The antenna maintains acceptable matching levels throughout the 4–8 GHz range, making it appropriate for mid-band microwave imaging systems. In terms of practical application, the selected frequency range is still highly relevant for breast cancer imaging, as microwave imaging systems often operate within specific sub-bands of the UWB spectrum depending on design trade-offs such as penetration depth and resolution.

The proposed antenna therefore provides a good balance between bandwidth, compactness, and performance. Overall, the results confirm that the proposed antenna achieves wide impedance bandwidth, strong resonance characteristics, and stable performance, making it a suitable candidate for breast cancer microwave imaging applications, even within a partial UWB range.

CONCLUSION

This study presented the design, fabrication and characterisation of a compact circularly slotted hexagonal antenna for potential application in microwave breast imaging. The proposed antenna was implemented on an FR-4 substrate with overall dimensions of 30 × 30 × 1.6 mm³. The reported results demonstrate an impedance bandwidth of approximately 4–8 GHz, corresponding to an absolute bandwidth of 4 GHz and a fractional bandwidth of 66.7%, with a minimum reflection coefficient (S_{11}) of approximately −27 dB near 5.5 GHz. The main contribution of this work is the development and experimental characterisation of a compact circularly slotted hexagonal antenna that provides wideband impedance performance within a portion of the conventional UWB spectrum. The comparison of simulated and measured reflection-coefficient responses provides antenna-level validation of the fabricated prototype. Nevertheless, the antenna does not cover the complete conventional UWB frequency range of 3.1–10.6 GHz, and the present work does not establish diagnostic accuracy or demonstrate reliable tumour detection through a fully validated microwave imaging system. Further limitations include the need for more comprehensive radiation-characteristic measurements, quantitative SAR assessment, mutual-coupling evaluation and validation using fully characterised tissue-mimicking phantoms. Future work should therefore focus on extending the operating bandwidth where required, evaluating electromagnetic exposure under appropriate conditions, and integrating the antenna into a complete microwave imaging system for measurements involving both tumour-free and tumour-containing breast phantoms, followed by image reconstruction and performance evaluation. These investigations will be necessary to establish the practical effectiveness of the proposed antenna in microwave breast-imaging applications.

Acknowledgement

This work is partially supported by the UK Engineering and Physical Sciences Research Council (EPSRC) under grant EP/Y035135/1, and HORIZON-MSCA-2022-SE-01-01-ID: 101131501, Marie Skłodowska-Curie, Research and Innovation Staff Exchange (RISE), titled: titled: 6G Terahertz Communications for Future Heterogeneous Wireless Network (6G-TERAFIT.

REFERENCES

Abdulla, F. A. A., & Demirkol, A. (2024) A novel textile-based.UWB patch antenna for breast cancer imaging. Physical an Engineering Sciences in Medicine, 47(3), 851–861.https://doi.org/10.1007/s13246-024-01409-w

Abdul-Al, M., et al. (2022). Wireless electromagnetic radiation assessment based on the specific absorption rate (SAR): A review case study. Electronics, 11(4), https://doi.org/511.

Aldelemy, A., et al. (2024). Monitoring bone healing: Integrating RF sensing with AI. IEEE Access.

Almuhlafi, A. M., Alshaykh, M. S., Alajmi, M., Alshammari, B., & Ramahi, O. M. (2024). A microwave differential dielectric sensor based on mode splitting of coupled resonators. Sensors, *24*(3), https://doi.org/1020.

Alanazi, M. D., Ali, W. A., Abdelhady, M., & Ibrahim, A. A. (2025). Millimeter-wave monopole antenna with circular polarization utilizing FSS polarizer for 5G communications. Engineering Science and Technology, an International Journal, 61, 101931.

Bangeles, J. M., Tapawan, E. M., & Arboleda, D. (2024). Wearable antennas in medical applications: A comprehensive review of design, performance, safety, and clinical applications. International Journal of Research Publication and Reviews, 5, https://doi.org/709–723.

Bayer Keskin, S. E., Koziel, S., & Szczepanski, S. (2025). Frequency reconfigurable PIN diode-based Reuleaux-triangle-shaped monopole antenna for UWB/Ku band applications. Scientific Reports, 15(1), https://doi.org/6555.

Belazzoug, M., et al. (2025). A compact 12-port MIMO dielectric lens antenna with wide-angle beam scanning for Ka-band applications. IEEE Open Journal of the Communications Society.

Danjuma, I. M., Akinsolu, M. O., See, C. H., Abd-Alhameed, R. A., & Liu, B. (2020). Design and optimization of a slotted monopole antenna for ultra-wide band body centric imaging applications. IEEE Journal of Electromagnetics, RF and Microwaves in Medicine and Biology, 4(2), https://doi.org/140–147.

Danjuma, I. M., et al. (2024). Rectangular slotted monopole antenna design for breast cancer tumor detection. In *2024* International Telecommunications Conference (ITC-Egypt) (pp. 672–676). https://doi.org/IEEE.

GuetaF, B. (2024). Design of a new antenna for biomedical applications.

Gupta, A., Saxena, P., Sharma, K., Kumar, M., & Bhardwaj, D. (2025). Role of di-electric materials as substrate for the performance of microstrip patch antenna: A review. In Advances in sustainable materials (pp. 363–376).

Haque, M. A., et al. (2024). Performance improvement of THz MIMO antenna with graphene and prediction bandwidth through machine learning analysis for 6G application. Results in Engineering, 24, https://doi.org/103216.

Huang, Y., et al. (2024). Space-based electromagnetic spectrum sensing and situation awareness. Space: Science & Technology, 4, https://doi.org/0109.

Kale, S. R., & Patil, D. P. (2024). A review of wearable antennas for 5G and body-centric wireless communication.

Kanagasabai, N. (2024). Radiation analysis of optimized wearable antenna sensor at 2.4 GHz on human body for WBAN applications. Informacije MIDEM, https://doi.org/54(4).

Khalid, B. (2023). Cancer detection using advanced UWB microwave technology. London South Bank University.

Lasemiimeni, Z., Atlasbaf, Z., & Karbaschi, N. (2021). Dual-functional ultrawideband antenna with high fidelity factor for body area networks and microwave imaging systems. IEEE Access, 9, https://doi.org/112930–112941.

Martellosio, A., et al. (2016). Dielectric properties characterization from 0.5 to 50 GHz of breast cancer tissues. IEEE Transactions on Microwave Theory and Techniques, 65(3), https://doi.org/998–1011.

Prasad, P. P. M., & Kanagasabai, N. (2024). Radiation analysis of optimized wearable antenna sensor at 2.4 GHz on human body for wireless body area network applications. Electronic Components and Materials, 54(4), https://doi.org/259–270.

Quraish, M. I., et al. (2024). Ultrawide band sensor design for early breast cancer detection. In 2024 International Telecommunications Conference (ITC-Egypt) (pp. 652–657). https://doi.org/IEEE.

Rafique, U., Pisa, S., Cicchetti, R., Testa, O., & Cavagnaro, M. (2022). Ultra-wideband antennas for biomedical imaging applications: A survey. Sensors, 22(9), https://doi.org/3230.

Rice, A., & Kiourti, A. (2022). High-contrast low-loss antenna: A novel antenna for efficient into-body radiation. IEEE Transactions on Antennas and Propagation, 70(11), https://doi.org/10132–10140.

Siaw, P. O., et al. (2024). Optmized metamaterial sensor for effective bone fracture detection. In 2024 International Telecommunications Conference (ITC-Egypt) (pp. 657–660). https://doi.org/IEEE.

Tong, C., Yang, N., Leung, K. W., & Liu, G. (2024). Design of MIMO antenna with DRAs and dual-function decoupling/radiating monopole antenna. IEEE Transactions on Antennas and Propagation.

Xinhua, P., et al. (2023). Uncertainty assessment of SAR measurement system. In 2023 IEEE 7th International Symposium on Electromagnetic Compatibility (ISEMC*)* (pp. 1–5). https://doi.org/IEEE.

Zaernia, A., Youseffi, M., Parisi, L., Abd-Alhameed, R., & Ma, R. (2024). A novel artificial intelligence-driven technique for enhancing medical imaging techniques to detect non-small cell lung cancer. In 2024 12th European Workshop on Visual Information Processing (EUVIP) (pp. 1–6). https://doi.org/IEEE.

Zhao, J., et al. (2022). Ultrawide bandwidth high-frequency ultrasonic transducers with gradient acoustic impedance matching layer for biomedical imaging. IEEE Transactions on Ultrasonics, Ferroelectrics, and Frequency Control, 69(6), https://doi.org/1952–1959
.

©2026 This is an Open Access article distributed under the terms of the Creative Commons Attribution 4.0 International license viewed via https://creativecommons.org/licenses/by/4.0/ which permits unrestricted use, distribution, and reproduction in any medium, provided the original work is cited appropriately.